Hindawi
Mobile Information Systems
Volume 2019, Article ID 9620153, 11 pages
https://doi.org/10.1155/2019/9620153

Research Article

Joint Time Switching and Transmission Scheduling for Wireless-Powered Body Area Networks

Jiaming Zhu[1], **Guopeng Zhang**[1], **Zongwei Zhu**[2], **and Kun Yang**[3]

[1]*School of Computer Science and Technology, China University of Mining & Technology, Xuzhou, China*
[2]*School of Software Engineering, University of Science & Technology of China, Hefei, China*
[3]*School of Computer Science and Electronic Engineering, University of Essex, Colchester, UK*

Correspondence should be addressed to Guopeng Zhang; zgpcumt@163.com

Received 29 July 2018; Revised 4 November 2018; Accepted 12 December 2018; Published 11 February 2019

Academic Editor: Paolo Bellavista

Outfitting humans with on-body/in-body sensor nodes, wireless body area networks (WBANs) are positioned as the key technology to enhance future telehealth service. The newly emerged wireless power transfer (WPT) and energy harvesting (EH) technology provides a potential of continuous power supply for WBANs. Since the radio frequency (RF) signals can carry energy as well as information at the same time, the time switching between the WPT phase and the wireless information transfer (WIT) phase should be carefully scheduled. By considering a telehealth application scenario (in which multiple patients coexist in a ward and each of them is monitored by multiple sensor nodes), this paper proposes to allocate the duty cycles for the WPT and WIT phases and schedule the transmission time for the WIT links in a joint manner. First, a frame structure for simultaneous information and power transfer (SWIPT) is designed over the time-and-spectrum domain. With the aim to satisfy the minimum rate demands of all the sensor nodes, the optimal duty time for the WPT phase and the optimal transmission time for the WIT links are jointly found by using the convex optimization technique. Finally, a fast algorithm is developed to search the optimal solution by introducing an admission control. The simulation results show that the proposed algorithm can effectively exploit the broadcasting property of RF energy radiation. If the network load were controlled below a certain level, the rate demands of all the sensor nodes in the network can be satisfied.

1. Introduction

Wireless body area network (WBAN) [1] is a key technology to enable information communication in next-generation patient-centric telehealth. Patients are outfitted with wearable, miniaturized, and low-power wireless sensor nodes. Body area information such as body vital signs, human motions, and surrounding environment status can be measured and wirelessly reported to telehealth providers or seamlessly integrated with patients' medical record without interrupting their normal activities [2]. Various wireless networking technologies and communication protocols such as IEEE 802.15.4 [3], ZigBee [4], Bluetooth Low Energy (BLE) [5], and Wi-Fi [6] have been designed as the options for short-range WBANs. Despite the improvement, two big intrinsic challenges still remain for WBANs, which are (1) the absence of ambient information related to the physiological data (which could introduce sensing cognition difficulty or even bias) and (2) battery life bottleneck incurred by wearable device proliferation [2].

In traditional battery-powered WBANs, sensor nodes only have batteries of limited capacity and it is inconvenient or even impossible to recharge or replace the batteries [7]. What is the more challenging is to fulfill the quality of service (QoS) of WBANs (such as data rate, latency, and reliability) which should be guaranteed against the channel fading caused by energy absorption, body movement, and multipath due to the surrounding environment of the human body [8]. Despite the technological improvements, the problem of continuous power supply for WBANs remains unsolved. However, in recent years, a newly emerged wireless power transfer (WPT) and energy harvesting (EH) technology for powering on-body/in-body sensor nodes becomes a promising solution to this problem [9]. Among various ways of EH, dedicated radio frequency (RF) energy sources do not depend on nature, such as wind, vibrations, and the sun; thus, they are more desirable for indoor health-monitoring purpose than other energy sources. With power beacons (PBs) [10] intentionally deployed to broadcast RF energy, sensor nodes housing circuits for harvesting RF energy can receive and utilize the energy for supporting the decoding and transmit circuits. The availability of in-exhaustible but unreliable RF energy sources changes the network designers' options considerably. Particularly, as RF signals can carry energy as well as information at the same time (which is referred to as simultaneous information and power transfer (SWIPT)), the time switching between the WPT links and WIT links should be carefully scheduled [11].

In this paper, we propose a resource allocation scheme to schedule the duty cycles of the WPT and WIT links in a joint manner. Specially, we investigate a typical e-healthcare application scenario, in which multiple patients coexist in a ward and each of them is monitored by multiple sensor nodes. The network QoS provision (in terms of the minimum transmission rate for each sensor node) is emphasized. Using a centralized algorithm framework, the optimal time switching strategy for the WPT and WIT links and the optimal transmission scheduling strategy for the sensor nodes are both obtained. It should be noted that the proposed solution of the wireless-powered BANs can also be applied to a variety of application scenarios. For example, it can be deployed in a sports ground or sports hall and, thus, can monitor the essential data of the athletes for analyzing and interpreting load, risk, wellness, training, health, testing, and performance anytime from anywhere. The main contributions of this paper are summarized as follows:

(1) An integrated data and energy frame structure (over the time-and-spectrum domain) is proposed for the SWIPT-based multiuser WBANs

(2) Under the promise to satisfy the minimum rate demands of all the on-body/in-body sensor nodes, the optimal duty time for the WPT links and the optimal transmission time for WIT links are jointly found by using the convex optimization technique

(3) By introducing an admission control mechanism, a fast algorithm is proposed to search the optimal solution of the joint WPT and WIT scheduling problem

The rest of this paper is organized as follows. The related works is reviewed in Section 2. Section 3 presents the system model. In Section 4, the SWIPT procedure for the investigated WBAN system is presented. In Section 5, we formulate the QoS guaranteed time switching and transmission scheduling as an optimization problem, and the problem is solved by using the convex optimization technique. Numerical results are provided in Section 6. Finally, Section 7 concludes this paper.

2. Related Works

WBANs deployed for continuously monitoring humans' health status and action pattern have got extensive usage owing to the technological progress on small-size, light-weight, ultra-low-power, and intelligent wearable devices. The monitoring occurs in a periodic manner, which requires relatively stable rates for applications' data uploading, while the latency can be leveraged on reliability and energy consumption. As battery charging or replacement is difficult for wireless sensor nodes, energy conservation is essential to maximize the lifetime of battery-powered WBANs. It is necessary to design suitable resource allocation and medium access control (MAC) mechanisms to provide higher network capacity, longer network lifetime, and adequate QoS [8].

With the aim to enhance energy efficiency, a great number of MAC protocols have been designed for generic wireless sensor networks (WSNs), and most of the special MAC protocols for WBANs are extended from the WSN MAC protocols. For instance, in order to support high traffic and low latency, Cascading Information retrieval by Controlling Access with Distributed slot Assignment (CICADA) protocol is developed in [12], which can immediately transmit data instead of buffering them locally. CICADA is a low-energy consumption protocol inherited from S-MAC [13]. By exploiting heartbeat rhythm information to achieve time synchronization, a TDMA-based MAC protocol is designed for WBANs in [14]. Sensor nodes are enabled to perform time synchronization by exacting heartbeat rhythm instead of relying on the radio component to receive periodic timing information from a central controller. Energy consumption can thus be largely reduced, and the network lifetime can be greatly prolonged. In general, the MAC protocols for WBANs are categorized into two types: (1) contention-based CSMA/CA protocols and (2) schedule-based TDMA protocols. In contention-based protocols [15, 16], the distributed sensor nodes use CSMA/CA to share the common channel which may result in a large amount of packet collision and energy consumption. In schedule-based TDMA protocols [7, 15, 16], a centralized controller is needed for time synchronization; thus, sensor nodes can be scheduled to transmit data in their own time slots. The packet collisions are avoided, and the energy consumption is reduced.

In battery-powered WBANs, recharging or replacing batteries for a large number of sensors is an unavoidable difficult problem. Harvesting RF energy from environment and converting it to usable electric energy can provide a continuous power supply for wireless sensor nodes. In ref. [17], the authors attempt to maximize the common throughput of all wireless nodes in a SWIPT network with a single RF source. In ref. [18], the placement of RF sources is optimized around the location of the wireless nodes. In ref. [19], based on a deterministic as well as a random energy harvesting model, the authors investigate how to maximize the data throughput in WBANs. In ref. [20], the authors propose an energy allocation water-filling method, and the optimal performance is achieved when the water levels of energy assume a staircase pattern. In ref. [21], the authors assume a block random EH model and also maximize the system throughput. Using effective dynamic programming and convex optimization method, the optimal solution for power allocation can be obtained.

With respect to the wireless-powered WBANs, the authors in ref. [22] study a point-to-point communication scheme, with the goal to maximize the data throughput from a sensor node to the access point (AP) in uplink. The main method is to balance the time duration among the command transfer phase, the WPT phase, and the WIT phase. In ref. [23], the authors study a wireless-powered WBAN with a helping relay. The relay can harvest RF energy sent by other nodes and then can use the harvested energy to help forward information to the destination. Both of the aforementioned studies [22, 23] only consider the point-to-point communication link in wireless-powered WBANs. In ref. [24], the authors propose a common-energy method with the aim to equalize the average energy harvested by sensor nodes in the WPT phase. However, only the single-user case is considered, in which only one patient carries multiple in/on body sensor nodes in the network. In addition, the issue of QoS provision which is essential in WBANs is not dealt with by the aforementioned studies [22–24].

Different from the prior studies [22–24], we consider a more practical WBAN, in which multiple patients coexist in a ward and each of them is monitored by multiple sensor nodes. Additionally, we emphasize the QoS provision (in terms of the minimum transmission rates) for the wireless-powered sensor nodes. As the first step in our research, the algorithm development and evaluation is the main objective of this paper. The issues of implementing the algorithm in current WBAN protocols as well as carrying experiments on available WPT and EH hardware and software are left to motivate our future work.

3. System Model

With the development of medical sensing devices, WBANs are ideally suitable for e-healthcare applications. The sensor nodes can be worn on or implanted in a patient's body, thus allowing for real-time data acquisition and information fusion and reporting. However, the limited battery capacity of the sensor nodes hits the bottleneck of the network lifetime. It is inconvenient even impossible to recharge or replace the batteries for wireless sensor nodes although they are featured by ultra-low-power wireless communications. The arrival of WPT and EH technology may break through the energy constraint, especially in an indoor setting (such as in a hospital ward) where reliable RF energy sources can continuously transfer RF energy to the sensor nodes. Therefore, in this paper, we investigate the issues related to the utilization of wireless-powered WBANs in an indoor environment as shown in Figure 1.

The considered hospital ward is of L meter long, W meter wide, and H meter height. There are K patients who are undergoing individual surgery with continuous health monitoring. The WBAN features one access point (AP) as the gateway to the Internet (which can collect information

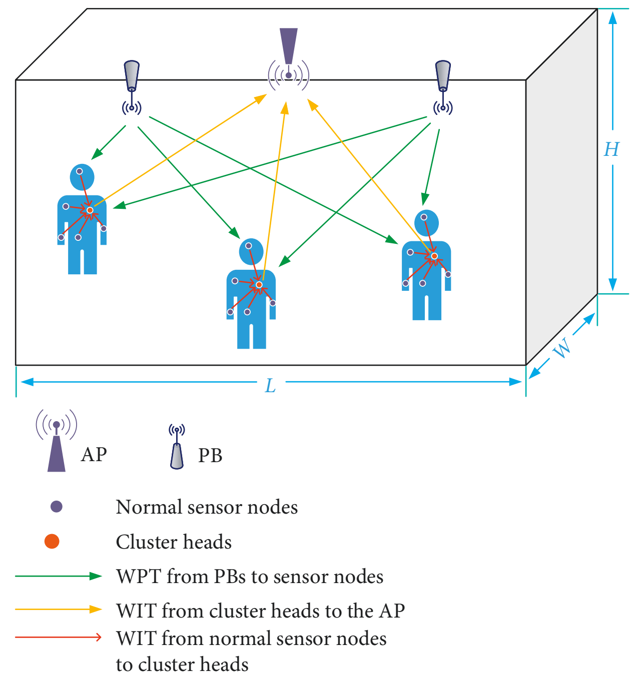

Figure 1: The system model of the considered wireless-powered WBAN.

from the sensor nodes and forwards the information to the remote healthcare application or system database) and a set $\mathcal{M}$ of M Power Beacons (PBs) as the RF energy sources. The AP and PBs are mounted on the ceiling of the ward and connected by power lines. We assume that there is a set $\mathcal{K}$ of K patients in the ward, and each kth ($\forall k \in \mathcal{K}$) patient is monitored by a set $\mathcal{N}_k$ of n_k sensor nodes. In order to reduce the traffic and energy cost, the WBAN is organized as a two-hop wireless network by grouping the sensor nodes into multiple clusters. The sensor nodes associated with a particular patient forms an independent cluster. In each kth cluster, a full function device (FFD) [13] is designated as the cluster head (CH), and the other $n_k - 1$ sensor nodes are treated as the reduced function device (RFD) [13] of the cluster. (In a general WSN, the network is clustered dynamically and the CHs are updated accordingly [25]. However, in a WBAN, the network is clustered according to the domain of a human body and the CHs are predefined devices with powerful computation and communication capabilities. Although a CH can be powered by rechargeable battery, this paper assumes that the CHs as well as the normal sensor nodes are all powered by the harvested RF energy. It should be noted that the CHs have the same sensing ability as the normal sensor nodes. For example, they can use accelerometers and gyroscopes to sensing the motion of a part of a human body and register and report the object's movement. The difference between the CHs and the normal sensor nodes is only from the data communication and processing perspective.) A normal sensor node can detect specific vital signs of a patient and then transmit the information to the CH. A CH, besides sensing the environment, is also responsible for collecting the information from the normal sensor nodes and forwarding the information to the AP (then to the medical service application). Without loss of generality, we label the CH in the kth cluster by $i = 1$ and the other $n_k - 1$ normal sensor nodes in the same cluster by $i = 2, \ldots, n_k$.

In the studied wireless-powered WBAN, there exist two types of links, i.e., the WPT links (from the PBs to the sensor nodes) and the WIT links (from the normal sensor nodes to the CHs and from the CHs to the AP). In order to save the scarce spectrum resource, we assume that the WPT links and the WIT links operate on the common frequency-band with bandwidth size of B Hz. The unit of resource allocation (over the time-and-spectrum domain) in the considered network is shown in Figure 2, which is termed as a resource block (RB) in this paper. In order to ease the analysis, we have normalized the duration of an RB to one.

Denote the instantaneous channel gain from the mth PB to the ith sensor node in the kth cluster by $g_{m,i}^k\ (\forall i \in \mathcal{N}_k)$, the instantaneous channel gain from the ith normal sensor node to the CH (in the same kth cluster) by $g_{i,1}^k\ (\forall i \in \mathcal{N}_k - \{1\})$, and the instantaneous channel gain from the CH to the AP by $g_{1,A}^k$. All the channels in the WBAN are assumed to be quasistatic flat fading. It means that $g_{m,i}^k$, $g_{i,1}^k$, and $g_{1,A}^k$ remain constant during one RB but can vary from one RB to another.

4. Energy and Information Transfer Mechanism

According to the aforementioned system settings, the designed SWIPT mechanism for the wireless-powered WBAN consists of the following three sequential phases: the WPT phase (wireless power transfer from the PBs to the sensor nodes), the first WIT phase (wireless information transfer from the normal sensor nodes to the CHs), and the second WIT phase (wireless information transfer from the CHs to the AP). The detail is described as follows.

4.1. The WPT Phase. Due to the additivity of the harvested RF energy at a receiver [26], the aggregate RF energy harvested from multiple PBs is additive for each EH node. The M PBs in this phase are scheduled by the resource scheduling center (RSC) to radiate RF energy simultaneously over the common frequency-band. Denote the duration of this phase by $\phi\,(0 < \phi \le 1)$, and denote the EH efficiency at the ith sensor node in the kth cluster by $\xi_i^k\,(0 < \xi_i^k < 1)$. The amount of the RF energy harvested by a sensor node can be given by

$$E_i^k = \xi_i^k \phi \sum_{m=1}^{M} P_m g_{m,i}^k, \quad \forall i \in \mathcal{N}_k, \text{ and } \forall k \in \mathcal{K}, \tag{1}$$

where the factor $\phi \sum_{m=1}^{M} P_m g_{m,i}^k$ is the total RF energy received by the sensor node before converting it into electric energy.

4.2. The First WIT Phase. In the WPT Phase, the sensor nodes replenish their energy. Then, in the first WIT phase, the normal sensor nodes in each cluster can transmit their detected information to the affiliated CH.

By using the TDMA technology, the first WIT phase is portioned into K nonoverlapped intervals which are then allocated by the RSC to the K clusters. Therefore, the severe intercluster and intracluster interference can be effectively avoided. Note that these K intervals are generally unequal, and we label them by $\theta_1, \theta_2, \ldots \theta_K$, respectively. The CH of each kth cluster then can conduct the secondary distribution by allocating τ_i^k time to the ith normal sensor node for WIT. Therefore, we have the following tight constraint:

$$\sum_{i \in \mathcal{N}_k - \{1\}} \tau_i^k = \theta_k, \quad \forall k \in \mathcal{K}. \tag{2}$$

It is assumed that the harvest-then-transmit (HT) protocol [15] is adopted in the network. Thus, each sensor node will use a fixed portion $\eta_i^k\,(0 < \eta_i^k < 1)$ of the harvested RF energy for WIT. As a result, the average transmission power at a sensor node is given by

$$p_i^k = \frac{\eta_i^k E_i^k}{\tau_i^k} = \eta_i^k \xi_i^k \phi \sum_{m=1}^{M} \frac{P_m g_{m,i}^k}{\tau_i^k}, \quad \forall i \in \mathcal{N}_k, \text{ and } \forall k \in \mathcal{K}, \tag{3}$$

where the factor $\xi_i^k \phi \sum_{m=1}^{M} P_m g_{m,i}^k$ is the total amount of RF energy harvested by a sensor node from all the M PBs.

Due to the WIT from a normal sensor node to the associated CH, the achievable data rate is given by

$$r_{i,1}^k = \tau_i^k B \log_2\left(1 + p_i^k \cdot \left(\frac{g_{i,1}^k}{\sigma^2}\right)\right), \quad \forall i \in \mathcal{N}_k - \{1\}, \text{ and } \forall k \in \mathcal{K}, \tag{4}$$

where σ^2 is the variance of the additive white Gaussian noise (AWGN) at a receiver.

4.3. The Second WIT Phase. Up to now, the CH of each cluster has acquired the sensed information of the associated normal sensor nodes. Then, in the 2nd WIT phase, the K CHs can upload the received information as well as their own information to the AP. For ease of analysis, we consider that neither data compression nor information fusion is applied at the CHs. Denote the transmission time allocated by the RSC to the CH of the kth cluster by τ_1^k. The average transmission power at the CH can then be given by

$$p_1^k = \frac{\eta_1^k E_1^k}{\tau_1^k}, \quad \forall k \in \mathcal{K}. \tag{5}$$

Due to the WIT from the kth CH to the AP, the achievable data rate is given by

$$r_{1,A} = \tau_1^k B \log_2\left(1 + p_1^k \cdot \left(\frac{g_{1,A}^k}{\sigma^2}\right)\right), \quad \forall k \in \mathcal{K}. \tag{6}$$

5. Problem Formulation

With the fast development of medical and sensing technology, various kinds of medical sensors are manufactured with different health monitoring purposes. This paper does not involve any specific health monitoring application but concentrates on meeting the real-time requirements of the

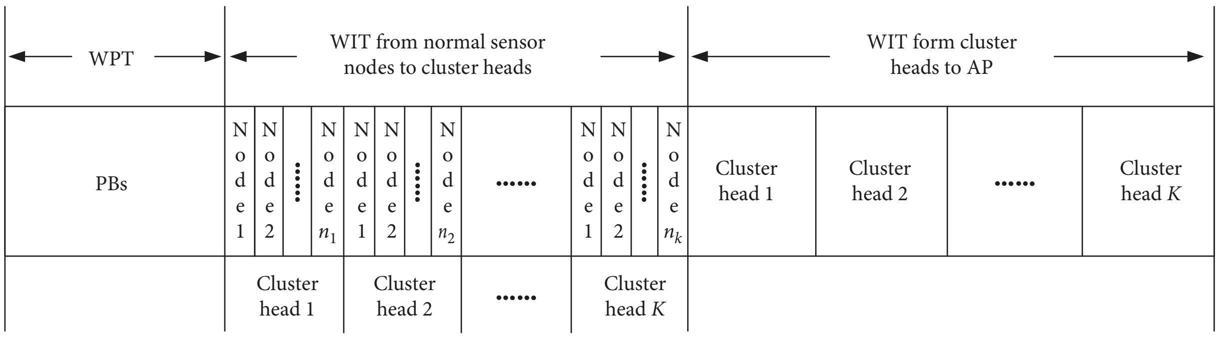

Figure 2: The designed structure of a resource block (RB) in the wireless-powered WBAN.

applications. For that purpose, we define the minimum rate requirement of a sensor node as b_i^k bits/RB ($\forall i \in \mathcal{N}_k$ and $\forall k \in \mathcal{K}$) and the total transmission time allocated to the kth cluster (including the CH and the normal sensor nodes in the cluster) as

$$\varepsilon^k = \tau_1^k + \sum_{i \in \mathcal{N}_k - \{1\}} \tau_i^k = \sum_{\forall i \in \mathcal{N}_k} \tau_i^k, \quad \forall k \in \mathcal{K}. \tag{7}$$

The objective of this paper is to exploit the available time and frequency resources and assist the network to maximize the total number of accepted clusters on a condition that the real-time requirements of all the served sensor nodes are satisfied. Mathematically, this problem is modeled as

$$\max K, \tag{8}$$

$$\text{s.t. } r_{i,1}^k = \tau_i^k B \log_2\left(1 + p_i^k \cdot \left(\frac{g_{i,1}^k}{\sigma^2}\right)\right) \geq b_i^k, \quad \forall i \in \mathcal{N}_k - \{1\}, \text{ and } \forall k \in \mathcal{K}, \tag{8.1}$$

$$r_{1,A} = \tau_1^k B \log_2\left(1 + p_1^k \cdot \left(\frac{g_{1,A}^k}{\sigma^2}\right)\right) \geq b_1^k + \sum_{i \in \mathcal{N}_k - \{1\}} b_i^k, \quad \forall k \in \mathcal{K}, \tag{8.2}$$

$$\phi + \sum_{k=1}^{K} \varepsilon^k = \phi + \sum_{\forall k \in \mathcal{K}} \sum_{\forall i \in \mathcal{N}_k} \tau_i^k \leq 1. \tag{8.3}$$

In constraint (8.1), the factor $\tau_i^k B \log_2(1 + p_i^k \cdot (g_{i,1}^k/\sigma^2))$ represents the achievable data throughput for a normal sensor node using time τ_i^k, while in constraint (8.2), the factor $\tau_1^k B \log_2(1 + p_1^k \cdot (g_{1,A}^k/\sigma^2))$ represents the achievable data throughput for the CH using time τ_1^k. Constraints (8.1) and (8.2) count for the demand of real-time transmission of the sensor nodes in the network. Finally, constraint (8.3) counts for the time constraint of an RB.

Problem (8) is a centralized optimization problem, as complete channel state information (abbreviated as CSI, which includes the information of channel states and transmission powers of all the WPT and WIT links in the WBAN) is required by the RSC to find the optimum. In what follows, we develop a fast algorithm to solve this problem. In order to satisfy the real-time requirements of the sensor nodes, an admission control mechanism is also designed.

5.1. Finding the Optimum. Due to the broadcasting property of wireless channels, the sensor nodes can harvest the RF energy radiated by multiple PBs over the common frequency-band simultaneously. Therefore, the duration of WPT in an RB (denoted by ϕ) is determined by the cluster which requires the longest WPT time to replenish the involved sensor nodes' energy. Based on this consideration, we can define the WPT time required by the kth cluster as ϕ^k, $\forall k \in \mathcal{K}$. If ϕ^k ($\forall k \in \mathcal{K}$) for all clusters were known, the optimal WPT time, i.e., the optimal point to switch from the WPT phase to the WIT phase in an RB, can be obtained as

$$\phi = \max\left\{\phi^k \,\middle|\, \forall k \in \mathcal{K}\right\}. \tag{9}$$

Next, we turn to find the optimal ϕ^k for $\forall k \in \mathcal{K}$. Firstly, in view of the quasistatic flat-fading property of the channels, we define the following constant factors (which remain constants at least in one RB) for ease of notation:

$$X_i^k = \eta_i^k \xi_i^k \sum_{m=1}^{M} P_m g_{m,i}^k, \quad \forall i \in \mathcal{N}_k, \text{ and } \forall k \in \mathcal{K}, \tag{10}$$

$$Y_i^k = \begin{cases} \dfrac{X_1^k \cdot g_{1,A}^k}{\sigma^2}, & i = 1, \\ \dfrac{X_i^k \cdot g_{i,1}^k}{\sigma^2}, & \forall i \in \mathcal{N}_k - \{1\}, \end{cases} \quad \forall k \in \mathcal{K}, \tag{11}$$

$$Z_i^k = \begin{cases} \dfrac{\sum_{\forall i \in \mathcal{N}_k} b_i^k}{B}, & i = 1, \\ \dfrac{b_i^k}{B}, & \forall i \in \mathcal{N}_k - \{1\}, \end{cases} \quad \forall k \in \mathcal{K}, \tag{12}$$

where X_i^k can be taken as the transmission power at the ith sensor node if the WPT interval were equal to the WIT interval, Y_i^k is thus the signal-to-noise ratio (SNR) at the receiver of the ith sensor node, and Z_i^k is the spectrum efficiency measured by the number of bits that can be conveyed by using on unit of the spectrum resource. By substituting equation (10) into equation (3), the average transmission power at a sensor node can be rewritten as

$$p_i^k = \frac{\phi^k}{\tau_i^k} X_i^k, \quad \forall i \in \mathcal{N}_k, \text{ and } \forall k \in \mathcal{K}. \tag{13}$$

Then, the mathematical problem for finding the optimal ϕ^k for $\forall k \in \mathcal{K}$ can be modeled as

$$\min_{\phi^k} \quad \varepsilon^k, \varepsilon^k = \sum_{\forall i \in \mathcal{N}_k} \tau_i^k, \tag{14}$$

$$\text{s.t.} \quad \tau_i^k \log_2\left(1 + \left(\frac{\phi^k}{\tau_i^k}\right) Y_i^k\right) \geq Z_i^k, \quad \forall i \in \mathcal{N}_k, \tag{14.1}$$

$$\phi^k + \sum_{\forall i \in \mathcal{N}_k} \tau_i^k \leq 1. \tag{14.2}$$

The property of problem (14) is summarized in Proposition 1.

Proposition 1. The optimization problem (14) is a convex optimization problem.

Proof. It is obvious that the objective function of problem (14) is affine and, thus, concave since it is a linear function of ϕ^k and τ_i^k ($\forall i \in \mathcal{N}_k$). Similarly, constraint (14.2) is also convex. Thus, we just need to verify the convexity of constraint (14.1). It is noted that X_i^k, Y_i^k, and Z_i^k are independent of ϕ^k and τ_i^k as indicated in equations (10)–(12). So, we can transform constraint (14.1) as

$$f\left(\phi^k, \tau_i^k\right) = Z_i^k - \tau_i^k \log_2\left(1 + \left(\frac{\phi^k}{\tau_i^k}\right) Y_i^k\right), \quad \forall i \in \mathcal{N}_k. \tag{15}$$

It is known that if the Hessian matrix of $f(\phi^k, \tau_i^k)$ is positive semidefinite, then it is convex [26]. By taking the second-order derivative of $f(\phi^k, \tau_i^k)$, the Hessian matrix can be given by

$$H = \begin{bmatrix} \dfrac{\partial^2 f}{\partial^2 \phi^k} & \dfrac{\partial^2 f}{\partial \phi^k \partial \tau_i^k} \\[2ex] \dfrac{\partial^2 f}{\partial \tau_i^k \partial \phi^k} & \dfrac{\partial^2 f}{\partial^2 \tau_i^k} \end{bmatrix} = \begin{bmatrix} \dfrac{\tau_i^k}{\ln 2}\left(\dfrac{Y_i^k/\tau_i^k}{1 + Y_i^k \phi^k/\tau_i^k}\right)^2 & -\dfrac{\phi^k}{\ln 2}\left(\dfrac{Y_i^k/\tau_i^k}{1 + Y_i^k \phi^k/\tau_i^k}\right)^2 \\[2ex] -\dfrac{\phi^k}{\ln 2}\left(\dfrac{Y_i^k/\tau_i^k}{1 + Y_i^k \phi^k/\tau_i^k}\right)^2 & \dfrac{1}{\ln 2}\left(\dfrac{Y_i^k/\tau_i^k}{1 + Y_i^k \phi^k/\tau_i^k}\right)^2 \end{bmatrix}. \tag{16}$$

It can be easily verified that the principal minors of matrix H are nonnegative, which means that matrix H is positive semidefinite. So, $f(\phi^k, \tau_i^k)$ is a convex function of ϕ^k and τ_i^k ($\forall i \in \mathcal{N}_k$).

As the objective function of problem (14) is concave and the constraint set is convex, we can now conclude that problem (12) is a convex optimization problem. □

Proposition 1. Ensures the existence of global optimal solutions to problem (14). The optimum can be found by using the following standard convex optimization method.

First, we introduce the Lagrangian function of problem (14) as

$$\mathcal{L}\left(\phi^k, \tau_i^k, \lambda_i, \mu\right) = \phi^k + \sum_{\forall i \in \mathcal{N}_k} \tau_i^k - \sum_{\forall i \in \mathcal{N}_k} \lambda_i \left(Z_i^k - \tau_i^k \log_2\left(1 + \left(\frac{\phi^k}{\tau_i^k}\right) Y_i^k\right)\right) - \mu\left(1 - \left(\phi^k + \sum_{\forall i \in \mathcal{N}_k} \tau_i^k\right)\right), \tag{17}$$

where λ_i ($\forall i \in \mathcal{N}_k$) and μ are the nonnegative Lagrangian multiplier.

Then, by applying the Karush–Kuhn–Tucker (KKT) optimality conditions [27], the optimal solution to problem (14) can be obtained by solving the following equation set:

$$\frac{\partial \mathcal{L}}{\partial \tau_i^k} = 1 + \lambda_i\left(\log_2\left(1 + \left(\frac{Y_i^k \phi^k}{\tau_i^k}\right)\right) - \frac{1}{\ln 2} \frac{Y_i^k \phi^k/\tau_i^k}{1 + \left(Y_i^k \phi^k/\tau_i^k\right)}\right) + \mu = 0, \quad \forall i \in \mathcal{N}_k, \tag{18.1}$$

$$\frac{\partial \mathcal{L}}{\partial \phi^k} = 1 + \frac{\lambda_i}{\ln 2} \frac{Y_i^k \phi^k}{\tau_i^k} + \mu = 0, \quad \forall i \in \mathcal{N}_k, \tag{18.2}$$

$$\lambda_i\left(\tau_i^k \log_2\left(1 + \frac{Y_i^k \phi^k}{\tau_i^k}\right) - Y_i^k\right) = 0, \quad \forall i \in \mathcal{N}_k, \tag{18.3}$$

$$\mu\left(1 - \left(\phi^k + \sum_{\forall i \in \mathcal{N}_k} \tau_i^k\right)\right) = 0, \quad \forall i \in \mathcal{N}_k. \tag{18.4}$$

Remark. It is noted that problem (14) can be solved by the CH of each cluster individually. The required information is only the CSI of the WPT and WIT links of the cluster members (including the CH and the normal sensor nodes), which can be transmitted by the PBs, the AP, and the normal sensor nodes to the CH through dedicated feedback channels. However, the solution to the aforementioned function set is difficult to find. An easy method to find ϕ^k for $\forall k \in \mathcal{K}$ is still required.

5.2. Fast Algorithm to Find ϕ^k. In order to find ϕ^k for $\forall k \in \mathcal{K}$, we further introduce a new parameter ϕ_i^k ($\forall i \in \mathcal{N}_k$ and $\forall k \in \mathcal{K}$), which represents the WPT time required by a sensor node to replenish the energy for the subsequent WIT phase in one RB. It is noted that the WPT time required by the kth cluster is determined by the sensor node which requires the longest WPT time to replenish the transmission energy. If ϕ_i^k for $\forall i \in \mathcal{N}_k$ in the kth cluster were known, the optimal ϕ^k for the cluster can then be determined by

$$\phi^k = \max\left\{\phi_i^k \,\middle|\, \forall i \in \mathcal{N}_k, \forall k \in \mathcal{K}\right\}. \tag{19}$$

Mathematically, the problem of finding optimal ϕ_i^k for $\forall i \in \mathcal{N}_k$ and $\forall k \in \mathcal{K}$ can be modeled as

$$\min_{\phi_i^k} \quad \pi_i^k, \pi_i^k = \phi_i^k + \tau_i^k, \tag{20}$$

$$\text{s.t.} \quad \tau_i^k \log_2\left(1 + \frac{\phi_i^k}{\tau_i^k} Y_i^k\right) = Z_i^k, \quad \forall i \in \mathcal{N}_k, \tag{20.1}$$

where the equality constraint (20.1) means that the minimum WPT time ϕ_i^k is obtained if Z_i^k bits are just transmitted successfully in an RB.

From equation (20.1), we can get

$$\phi_i^k = \left(2^{Z_i^k/\tau_i^k} - 1\right)\frac{\tau_i^k}{Y_i^k}. \tag{21}$$

By substituting equation (21) into the objective function of problem (20), we can get

$$\pi_i^k = \left(2^{Z_i^k/\tau_i^k} - 1\right)\frac{\tau_i^k}{Y_i^k} + \tau_i^k. \tag{22}$$

Obviously, the minimum π_i^k can be obtained when the first derivative equals to zero. Accordingly, by solving the following equation:

$$\begin{aligned}\frac{\partial \pi_i^k}{\partial \tau_i^k} &= \left(\tau_i^k\right)^3 - Y_i^k \tau_i^k \left(2^{Z_i^k/\tau_i^k} - 1\right) \\ &\quad - \ln 2 Y_i^k Z_i^k \left(2^{Z_i^k/\tau_i^k} - 1\right) = 0, \quad \forall i \in \mathcal{N}_k,\end{aligned} \tag{23}$$

we can get the optimum ϕ_i^k for $\forall i \in \mathcal{N}_k$ and $\forall k \in \mathcal{K}$.

Remark. Equation (23) is an exponential equation with one unknown parameter τ_i^k, and there is no analytical solution. In this paper, we use the exhaustive searching algorithm of discretization to solve this equation. With this design, we first discretize the available time for resource allocation into a finite number of V time slots, each with duration $\Delta = 1/V$. The time duration Δ is chosen to be sufficiently small, such that the error to the optimal value is below a given threshold. Once equation (23) were solved, ϕ^k can then be obtained by using equation (19). Therefore, this algorithm is of liner complexity and can be practically implemented for WBANs of a moderate number of sensor nodes.

5.3. Admission Control Mechanism. As a summary, the proposed joint time switching and transmission scheduling (JTS) algorithm (Algorithm 1) for the considered wireless-powered WBAN is given below.

Remark. It should be noted that the performance of the proposed resource allocation and scheduling algorithm is only affected by the time-variant channel coefficients of the involved sensor nodes, power beacons, and access point. As the wireless channels in body area networks are assumed to be slow flat fading, these parameters remain constant during one scheduling period. Along with the movement of the human body, the channel coefficients $g_{m,i}^k$, $g_{i,1}^k$, and $g_{1,A}^k$ (defined in equations (1), (4), and (6), respectively) may vary from one period to another. Therefore, the proposed Algorithm 1 should be carried out in a period-by-period manner in answer to the channel state changes.

6. Simulation Results

In order to testify the resource management and QoS assurance capabilities, this section shows the simulation results of the proposed time switching and transmission scheduling scheme. The simulated wireless-powered WBAN is illustrated in Figure 1, in which multiple patients are monitored by a number of on-body/in-body sensor nodes in a hospital ward of 10 m long, 10 m wide, and 3 m height. The unique AP is mounted on the center of the ward ceiling, and the coordinate is (5 m, 5 m, 3 m). Two dedicated PBs as RF energy sources are also deployed in the ceiling of the ward. Their coordinates are (3.3 m, 3.3 m, 3 m) and (6.6 m, 6.6 m, 3 m), respectively. The bandwidth size of the network is 1 MHz. The noise variance of the channel is set as $\sigma^2 = 10^{-11}$, and the power-law path-loss of the channel is modeled as $1/d^4$, where d is the distance from a transmitter to the receiver. The body shadowing is modeled as a Gauss-distributed random variable with zero mean and variance 15 dB [24].

In order to match the actual situation of current WPT and EH hardware, we refer to the Powercast products [28] to set the simulation parameters. Powercast is the pioneer of RF-based long-range WPT and EH technology. According to the product datasheet, the amount of the transmittable power for the Powercaster Transmitter TX91501 is limited to 4 watts EIRP [29], and the RF-to-DC conversion efficiency of the Powerharvester Receiver is as high as 75% [30]. These enable an operating range of 12–14 meters line of sight. According to the performance of existing products, we set the transmission power of each PB as −20 dB. For each EH sensor node, we assume that the energy-harvesting efficiency is 0.5, and the portion of the harvested energy used for WIT is 0.5.

6.1. Case 1: Fixed Number of Patients with Varied Number of On-Body/In-Body Sensors. In the first experiment, we fix the number of the patients in the ward as $K = 4$ and the number of the normal sensor nodes on/in each patient is increased from 2 to 20. The coordinates of the patients are (1 m, 1 m, 0 m), (3.7 m, 3.7 m, 0 m), (6.3 m, 6.3 m, 0 m), and (9 m, 9 m, 0 m), respectively. The sensor nodes are randomly distributed throughout a patient, and their minimum rate requirements are set as 50 Kb/RB. The experiment is performed 10^4 times in order to average out the effects of the body shadowing. The duty time scheduled to the WPT phase as well as the WIT phase in one RB is shown in Figure 3.

Step 1 (initialization): All the normal sensor nodes in each kth cluster, $\forall i \in \mathcal{N}_k - \{1\}$ and $\forall k \in \mathcal{K}$, send their CSI and the rate requirement b_i^k to the CH of the kth cluster through the dedicated feedback channel. Then, the CSI and the rate requirement information of the normal sensor nodes and the CHs are conveyed to the RSC also through the dedicated feedback channel.
Step 2: By solving equations (21) and (23), the RSC can obtain ϕ_i^k, i.e., the minimum WPT time required by the ith ($\forall i \in \mathcal{N}_k - \{1\}$ and $\forall k \in \mathcal{K}$) normal sensor node in each kth cluster.
Step 3: By using equation (19), the RSC can determine ϕ^k; i.e., the minimum WPT time required by the kth ($\forall k \in \mathcal{K}$) cluster is determined.
Step 4: After acquiring ϕ^k ($\forall k \in \mathcal{K}$), the RSC can determine ϕ, i.e., the minimum WPT time for the WBAN by using equation (9).
Step 5: Upon obtaining ϕ, the RSC can use equations (1), (3), (4), and (6) to recalculate the minimum transmission time $\widehat{\tau}_i^k$ ($\forall i \in \mathcal{N}_k$ and $\forall k \in \mathcal{K}$) required by each sensor node in the BAN.
Step 6 (admission control): The RSC testifies whether the real-time requirement of all the sensor nodes (i.e., $\phi + \sum_{\forall k \in \mathcal{K}} \sum_{\forall i \in \mathcal{N}_k} \tau_i^k \leq 1$ in constraint (8.3)) is satisfied. If yes, then go to *Step 7*. Otherwise, the $\bar{k}$th cluster ($\bar{k} = \arg_{\forall k \in \mathcal{K}} \max (\phi^k + \sum_{\forall i \in \mathcal{N}_k} \widehat{\tau}_i^k)$) which requires the maximum WPT and WIT time will be delayed to access the network. After updating $\widehat{\mathcal{K}} = \mathcal{K} - \{\bar{k}\}$, the algorithm goes back to *Step 4* until the real-time requirement of all the sensor nodes is satisfied.
Step 7: According to the aforementioned resource allocation result, including the admitted cluster set $\widehat{\mathcal{K}}$, the optimal WPT time ϕ, and the optimal WIT time $\widehat{\tau}_i^k$ ($\forall i \in \mathcal{N}_k$ and $\forall k \in \mathcal{K}$), the RSC can thus schedule the network resource to the WPT and WIT links. The scheduling information is firstly fed back to the PBs and the CHs by the RSC. Then, it is further conveyed to the normal sensor nodes by the CHs.

Algorithm 1: The proposed JTS algorithm for wireless-powered WBAN.

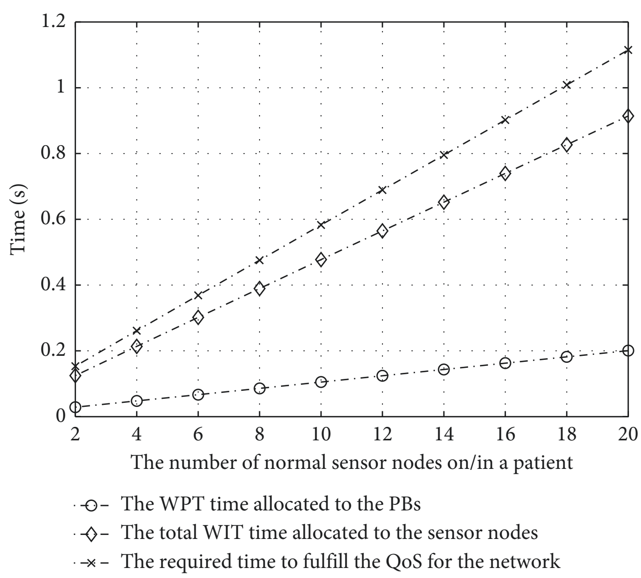

Figure 3: The duty times of the WPT and WIT phases versus the number of the sensor nodes on/in a patient.

From Figure 3, we can observe that, with the increment of the number of the sensor nodes on/in each patient, the WPT time (dashed curve with circles) required to replenish their energy and the total WIT time (dashed red curve) required to uploading their sensing data increase linearly. In comparison to duty time of the WPT phase, the duty time of the WIT phase accounts for the most part of the time to fulfill the minimum rate requirements (dashed blue curve). This implies that the PBs radiating with low power are feasible for WBANs, since the sensor nodes in WBANs are with periodic low traffic load (below 50 Kb/RB).

From Figure 3, we also note that when the number of sensor nodes on each patient is larger than 18, their minimum rate requirements (50 Kb/RB) cannot be satisfied by the network because the total WPT and WIT time (dashed blue curve) required to fulfill the minimum rate requirements is larger than the duration of an RB (normalized to 1). In such a situation, the admission control should be applied; thus, some of the sensor nodes are to be delayed to access the network.

Next, in order to show the QoS assurance capability of the proposed scheme, we fix the number of the sensor nodes in/on each patient at 17, and the acquired data rates of all the sensor nodes are shown in Figure 4.

From Figure 4, we note that the minimum rate requirements of all the sensor nodes are satisfied, especially for the cluster head nodes, which not only transmit their own data to the AP but also relay the sensing data of the affiliated normal sensor nodes to the AP. The simulation results imply that if the network load were controlled below a certain level, the QoS demand of the sensor nodes can be satisfied by the proposed scheme.

6.2. Case 2: Fixed Number of On-Body/In-Body Sensors with Varied Number of Patients.

In this experiment, we vary the number of the patients in the ward from $K = 1$ to 12, each patient carrying one cluster head node and 10 normal sensor nodes. The patients are randomly located along the straight line from (1 m, 1 m, 0 m) to (9 m, 9 m, 0 m) in the ward. The minimum rate requirements of the sensor nodes are set as 50 Kb/RB. The simulation result is shown in Figure 5.

From Figure 5, we note that, with the increment of the number of the patients in the ward, the total WIT time (dashed curve with diamonds) required by the sensor nodes to uploading their sensing data increases linearly. It is resultant from the TDMA-based channel accessing method, by which each sensor node should be allocated nonoverlapped time for data transmission. However, the WPT time (dashed green curve) required to replenish the energy of the sensor nodes remains unchanged with the varied number of patients. It indicates that the proposed scheme can effectively exploit the broadcasting property of the RF energy radiation.

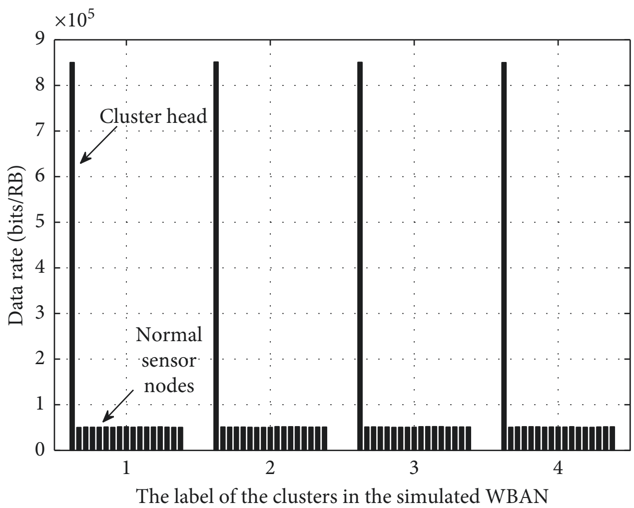

Figure 4: The achievable data rates of all the sensor nodes.

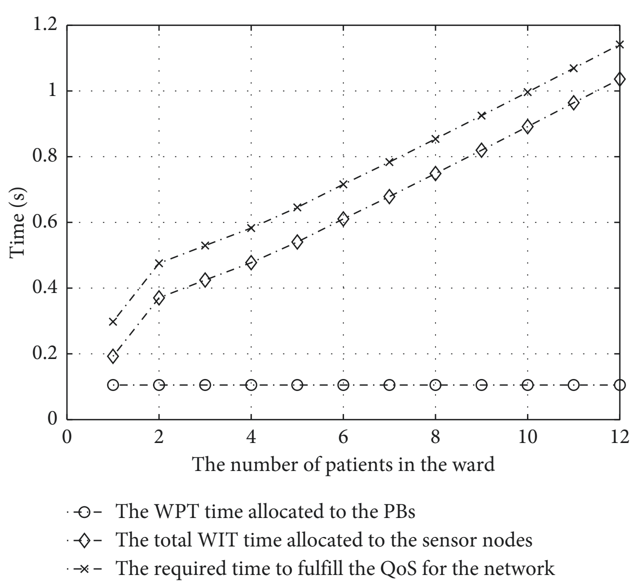

Figure 5: The duty times of the WPT and WIT phases versus the number of the patients in the ward.

From Figure 5, we also note that when the number of the patients is larger than 10, the minimum rate requirement (50 Kb/RB) of the sensor nodes cannot be satisfied. The admission control should be applied in such a situation again. We fix the number of the patients at 10 and show the acquired data rates of all the sensor nodes in Figure 6. It verifies that the minimum rate requirements of the normal sensor nodes as well as the cluster head nodes can be satisfied by the proposed scheme.

6.3. Case 3: Fixed Number of Patients and On-Body/In-Body Sensors with Varied Rate Requirements. In the last experiment, we testify the QoS assurance ability of the proposed scheme in providing different data rates for the served sensor nodes. For that purpose, we fix the number of the patients in the ward at 4 and the number of the sensor nodes on/in each

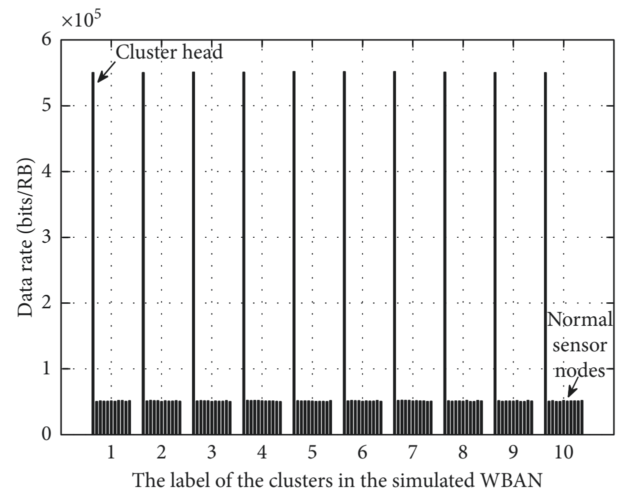

Figure 6: The achievable data rates of all the sensor nodes.

patient at 11, but we increase the minimum rate requirements of the sensor nodes from 10 Kb/RB to 100 Kb/RB. The simulation result is shown in Figure 7.

From Figure 7, we note that, with the increment of the minimum rate requirements, the duty times of the WPT phase (dashed curve with circles) and the WIT phase (dashed curve with diamonds) increase linearly. The reason is that each sensor node should be allocated more transmission time to achieve the increased data rate. As a result, more WPT time should be reserved for the sensor nodes in order to equalize the increased energy consumption for the subsequent WIT phase.

From Figure 7, we observe again that when the minimum rate requirement of each sensor node is larger than 80 Kb/RB, the requirements cannot be satisfied by the network. Thus, the admission control should be applied to delay some of the sensor nodes to access the network. Finally, in Figure 8, we show the acquired data rates of all the sensor nodes when the minimum rate requirement is 80 Kb/RB. It verifies that the QoS demand of the sensor nodes can be satisfied by the proposed scheme even in a close-to-saturation network situation.

7. Conclusions

In this paper, we propose a joint time switching and transmission scheduling scheme in wireless-powered WBANs. To implement the simultaneous information and power transfer, we divide a basic resource block of the network into three phases, i.e., the WPT phase (used for replenishing energy for the sensor nodes), the first WIT phase (used for data transmission from the normal sensor nodes to the cluster header nodes), and the second WIT phase (used for data transmission from the CHs to the AP). In order to satisfy the minimum rate requirements of the on-body/in-body sensor nodes, the optimal duty cycle for the WPT phase and the optimal transmission times for the WIT links are found. The simulation results show the abilities of the proposed scheme in QoS assurance and exploiting the broadcasting property of the RF energy radiation.

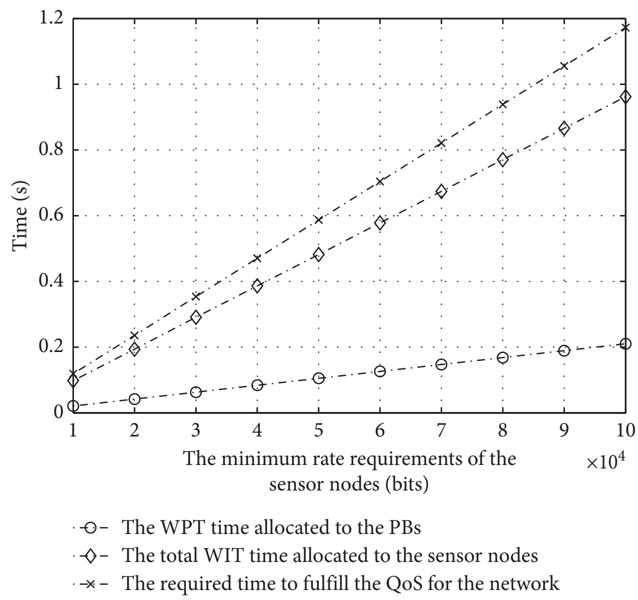

Figure 7: The duty times of the WPT and WIT phases versus the different rate requirements.

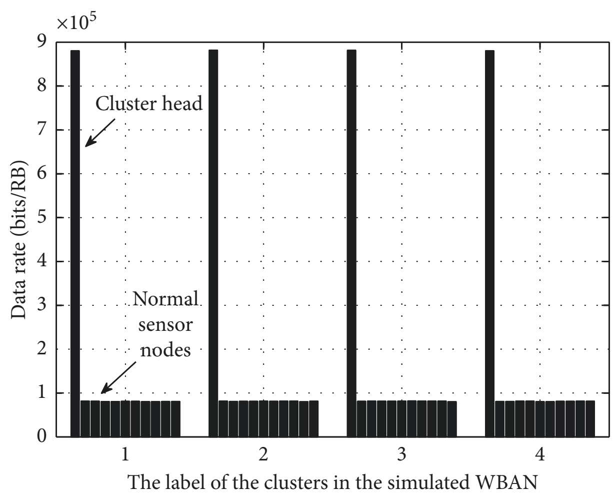

Figure 8: The achievable data rates of all the sensor nodes.

Data Availability

The simulation codes used to support the findings of this study are available from the corresponding author upon request, or can be accessed by downloading the [simulation codes.zip] file at the following website: http://www.scholat.com/portalPaperInfo.html?paperID=36995&Entry=gpzhang.

Conflicts of Interest

The authors declare that they have no conflicts of interest.

Acknowledgments

This work was supported in part by the Fundamental Research Funds for the Central Universities of China (Grant no. 2015XKQY18) and the National Natural Science Foundation of China (Grant nos. 61572389 and 61620106011).

References

[1] S. Movassaghi, M. Abolhasan, J. Lipman, D. Smith, and A. Jamalipour, "Wireless body area networks: a survey," *IEEE Communications Surveys and Tutorials*, vol. 16, no. 3, pp. 1658–1686, 2014.

[2] N. Zhu, T. Diethe, M. Camplani et al., "Bridging e-Health and the Internet of Things: the SPHERE Project," *IEEE Intelligent Systems*, vol. 30, no. 4, pp. 39–46, 2015.

[3] J. A. Gutierrez, M. Naeve, E. Callaway, M. Bourgeois, V. Mitter, and B. Heile, "IEEE 802.15.4: a developing standard for low-power low-cost wireless personal area networks," *IEEE Network*, vol. 15, no. 5, pp. 12–19, 2001.

[4] K. Gill, S.-H. Yang, F. Yao, and X. Lu, "A zigbee-based home automation system," *IEEE Transactions on Consumer Electronics*, vol. 55, no. 2, pp. 422–430, 2009.

[5] X. Fafoutis, E. Tsimbalo, and R. Piechocki, "Timing channels in Bluetooth low energy," *IEEE Communications Letters*, vol. 20, no. 8, pp. 1587–1590, 2016.

[6] Y. Wang, Q. Wang, Z. Zeng et al., "WiCop: engineering WiFi temporal white-spaces for safe operations of wireless body area networks in medical applications," in *Proceedings of Real-Time Systems Symposium*, pp. 170–179, Vienna, Austria, November-December 2011.

[7] B. Liu, Z. Yan, and C. W. Chen, "MAC protocol in wireless body area networks for E-health: challenges and a context-aware design," *IEEE Wireless Communications*, vol. 20, no. 4, pp. 64–72, 2013.

[8] M. Chen, S. Gonzalez, A. Vasilakos, H. Cao, and V. C. M. Leung, "Body area networks: a survey," *Mobile Networks and Applications*, vol. 16, no. 2, pp. 171–193, 2010.

[9] E. Ibarra, A. Antonopoulos, E. Kartsakli, J. J. P. C. Rodrigues, and C. Verikoukis, "QoS-Aware energy management in body sensor nodes powered by human energy harvesting," *IEEE Sensors Journal*, vol. 16, no. 2, pp. 542–549, 2016.

[10] Y. Li, R. Wang, X. Liao, and S. Zhu, "Optimal multiuser scheduling for wireless powered communication systems," in *Proceedings of IEEE International Conference on Communications (ICC 2016)*, pp. 1–6, Kuala Lumpur, Malaysia, May 2016.

[11] X. Di, K. Xiong, P. Fan, and H. Yang, "Simultaneous wireless information and power transfer in cooperative relay networks with rateless codes," *IEEE Transactions on Vehicular Technology*, vol. 66, no. 4, pp. 2981–2996, 2016.

[12] B. Latr, B. Braem, I. Moerman et al., "A low-delay protocol for multihop wireless body area networks," in *Proceedings of International Conference on Mobile and Ubiquitous Systems: Networking and Services*, pp. 1–8, Philadelphia, PA, USA, March 2007.

[13] W. Ye, J. Heidemann, D. Estrin et al., "Medium access control with coordinated adaptive sleeping for wireless sensor networks," *IEEE/ACM Transactions on Networking*, vol. 12, no. 3, pp. 493–506, 2004.

[14] H. Li and J. Tan, "Heartbeat-driven medium-access control for body sensor networks," *IEEE Transactions on Information Technology in Biomedicine*, vol. 14, no. 1, pp. 44–51, 2010.

[15] A. Boulis and Y. Tselishchev, "Contention vs. Polling: a study in body area networks MAC design," in *Proceedings of 5th International Conference Body Area Networks (BodyNets 2010)*, pp. 151–157, Corfu, Greece, September 2010.

[16] M. A. Ameen, J. Liu, S. Ullah, and K. S. Kwak, "A power efficient MAC protocol for implant device communication in wireless body area networks," in *Proceedings of 2011 IEEE Consumer Commun. And Networking Conference (CCNC)*, pp. 1155–1160, Las Vegas, NV, USA, January 2011.

[17] H. Ju and R. Zhang, "Throughput maximization in wireless powered communication networks," *IEEE Transactions on Wireless Communications*, vol. 13, no. 1, pp. 418–428, 2014.

[18] X. Liu, F. Hu, W. Xiong, Y. Du, and L. Cen, "Sparse array synthesis for WBAN with minimised side lobe via convex optimisation," *IET Communications*, vol. 10, no. 17, pp. 2452–2460, 2016.

[19] J. Yang and S. Ulukus, "Optimal packet scheduling in an energy harvesting communication system," *IEEE Transactions on Communications*, vol. 60, no. 1, pp. 220–230, 2012.

[20] O. Ozel, K. Tutuncuoglu, J. Yang, S. Ulukus, and A. Yener, "Transmission with energy harvesting nodes in fading wireless channels: optimal policies," *IEEE Journal on Selected Areas in Communications*, vol. 29, no. 8, pp. 1732–1743, 2011.

[21] C. K. Ho and R. Zhang, "Optimal energy allocation for wireless communications with energy harvesting constraints," *IEEE Transactions on Signal Processing*, vol. 60, no. 9, pp. 4808–4818, 2012.

[22] Z. Ling, F. Hu, L. Wang, J. Yu, and X. Liu, "Point-to-point wireless information and power transfer in WBAN with energy harvesting," *IEEE Access*, vol. 5, pp. 8620–8628, 2017.

[23] L. Wang, F. Hu, Z. Ling, and B. Wang, "Wireless information and power transfer to maximize information throughput in WBAN," *IEEE Internet of Things Journal*, vol. 4, no. 5, pp. 1663–1670, 2017.

[24] J. C. Kwan and A. O. Fapojuwo, "Radio frequency energy harvesting and data rate optimization in wireless information and power transfer sensor networks," *IEEE Sensors Journal*, vol. 17, no. 15, pp. 4862–4874, 2017.

[25] J. C. Haartsen, "The Bluetooth radio system," *IEEE Personal Communications*, vol. 7, no. 1, pp. 28–36, 2000.

[26] S. He, J. Chen, F. Jiang et al., "Energy provisioning in wireless rechargeable sensor networks," *IEEE Transactions on Mobile Computing*, vol. 12, no. 10, pp. 1931–1942, 2012.

[27] S. Boyd and L. Vandenberghe, *Convex Optimization*, Cambridge University Press, Cambridge, UK, 2004.

[28] https://www.powercastco.com/.

[29] http://www.powercastsensors.com/files/TX91501-datasheet.pdf.

[30] https://www.powercastco.com/products/powerharvester-receivers.